Pre-Clinical Research Report

Journal of INTERNATIONAL MEDICAL RESEARCH

Journal of International Medical Research
48(10) 1–9

DOI: 10.1177/0300060520966884
journals.sagepub.com/home/imr
SAGE

Biomechanical evaluation of axial-loading simulated experiment in wrist fractures: a finite element analysis

You-Liang Fan[1], Hai-Yun Xu[1], Ming-Yang Xia[1], Wen Zhang[2], Hui-Long Wen[1], Li-Bo Gao[1] and Yan-Hui Pei[1]

Abstract

Objective: To assess the biomechanical properties that influence wrist fracture, so as to provide the theoretical basis for simulation experiments to aid the optimal design of wrist protectors.

Methods: Six cadaveric wrists were included as experimental specimens. Wrist specimens wearing wrist protectors formed the experimental group and unprotected wrist specimens formed the control group. The wrist specimens were axially loaded under physiological loads and the stress magnitude and distribution of the experimental and control groups were obtained. A three-dimensional wrist finite element model of a healthy volunteer was developed to verify the rationality and effectiveness of the cadaveric wrist models.

Results: Under normal physiological loads, the stress on the radioulnar palmar unit was high and manifested in the form of pressure, while the stress on the radioulnar dorsal unit was lower and manifested in the form of tension. The stresses on the radial distal palmar, ulnar distal palmar, radial distal dorsal, ulnar distal dorsal, radial proximal palmar and ulnar proximal palmar units in the experimental group were less than those in the control group.

Conclusion: Under physiological loads, wearing a wrist protector can reduce the stress on the radioulnar distal palmar, radioulnar proximal palmar and radioulnar distal dorsal units, while having no obvious effect on the radioulnar proximal dorsal units.

[1]Department of Orthopaedics, Changzhou Fourth People's Hospital (Changzhou Cancer Hospital Affiliated to Soochow University), Changzhou, Jiangsu Province, China
[2]Department of Orthopaedics, Orthopaedic Institute, Soochow University, Suzhou, Jiangsu Province, China

Corresponding author:
Yan-Hui Pei, Changzhou Fourth People's Hospital (Changzhou Cancer Hospital Affiliated to Soochow University), 68 Honghe Road, Changzhou 213032, Jiangsu Province, China.
Email: wjpyh2001@163.com

Keywords
Wrist fracture, biomechanical evaluation, finite element analysis, wrist protector

Date received: 6 May 2020; accepted: 25 September 2020

Introduction

The incidence of wrist fracture is widespread, currently accounting for 6.7–11.0% of total body fractures, which inevitably results in high medical costs.[1,2] The wrist joint is mainly composed of a bony structure and other small joints, forming a composite joint between the forearm and palm.[3,4] Moreover, the bony structure and small joints have a clear division of labour in terms of structure.[5,6] As the most complicated joint in the human body,[7] the mechanical mechanism of the wrist joint is complicated. Once the wrist joint is injured, it is likely to cause secondary damage to other wrist structures,[8] affecting the function of relevant parts of the upper limbs. Thus, a thorough and detailed study of the wrist joint is clinically significant.

Currently, research on the prevention of wrist fractures remains limited to drugs to treat osteoporosis and osteoporotic fractures predicted by quantitative computed tomography.[9–12] However, from the perspective of biomechanics and finite element analysis (FEA), it is of great practical significance to explore the prevention and treatment of wrist fractures. Based on this, the current study combined mechanical experiments on cadaveric wrists and finite element wrist simulation analysis to provide the theoretical basis for simulation experiments of wrist fracture in order to aid the optimal design of wrist protectors.

Materials and methods

Models and materials

Six wrist samples were collected from cadavers with an age at mortality of 20–50 years at the Department of Human Anatomy Medicine, Soochow University, Soochow, Jiangsu Province, China. The wrist samples underwent X-ray examination and bone mineral density (BMD) measurements in order to exclude skeletal defects, dislocations, lesions and tumours prior to storage at –20 °C. An open cuboidal container made of stainless steel (80 mm × 80 mm × 100 mm) was designed to hold the wrist samples. Bone cements with low viscosity (PALACOS® bone cements; Heraeus Medical, Wehrheim, Germany) were used to fix the wrist samples vertically in the cuboidal container so that the wrist samples were firmly fixed without any movement (Figure 1).[13] Furthermore, the wrist samples were attached to a stress sensing system device (Huangyan Corporation, Taizhou, China), a microelectronic universal testing machine (Shijin Corporation, Jinan, China) and four static strain test units (Shijin Corporation), which were connected by wires. Four static strain test units were respectively marked as A, B, C and D units, of which unit A represented the stress of the radioulnar distal palmar unit; unit B represented the stress of the radioulnar distal dorsal unit; unit C represented the stress of the radioulnar proximal palmar unit; and unit D represented the stress of the radioulnar proximal dorsal unit.

Computed tomography (CT) data were obtained from a 30-year-old healthy Chinese male volunteer, whose age and forearm size strictly matched the requirements of the above cadaveric specimens. In order to ensure the normal anatomy of the wrist, an X-ray of the wrist was performed to exclude fractures, lesions and

other conditions. The experimental devices that were used in this current study included a dual-source CT scanner (Siemens, Berlin, Germany), a computer (Dell, Round Rock, TX, USA), Mimics 19.0 software (Materialise, Leuven, Belgium), Geomagic Studio 12.0 software (Raindrop Geomagic, Research Triangle, NC, USA) and Abaqus 6.51 software (Dassault Simulia, Providence, RI, USA).

Ethical approval was obtained from the Institutional Review Board of Changzhou Fourth People's Hospital (no. 20171015) and written informed consent was obtained from the volunteer.

Biomechanical testing methods

The biomechanical experiment in this study was an impact test using static loading within the yield strength and the mechanical property was within the normal physiological range. Wrist specimens wearing wrist protectors formed the experimental group and unprotected wrist specimens formed the control group. In the experimental group, the wrist protectors were made of 20-mm thick, soft sponge materials and 2-mm thick polypropylene hard materials. Then, the mode of mechanical axial compression was selected, the strain sensing system on the wrist models was installed and the static resistance strain gauges were further connected, so as to prepare for the next phase of the experiment. With the palm facing upward, the wrist models were fixed at 90° perpendicular to the floor and the pressure hammer was aimed at the centre of the navicular and lunar bone. The initial loading speed was set at 2 mm/min and the loading range was 0–600 N (Figure 1). The strain values of all target units were recorded for every 20 N load and each specimen was tested three times under the same conditions.

Construction of a 3D finite element model

The volunteer underwent transverse CT scanning that ranged from the proximal

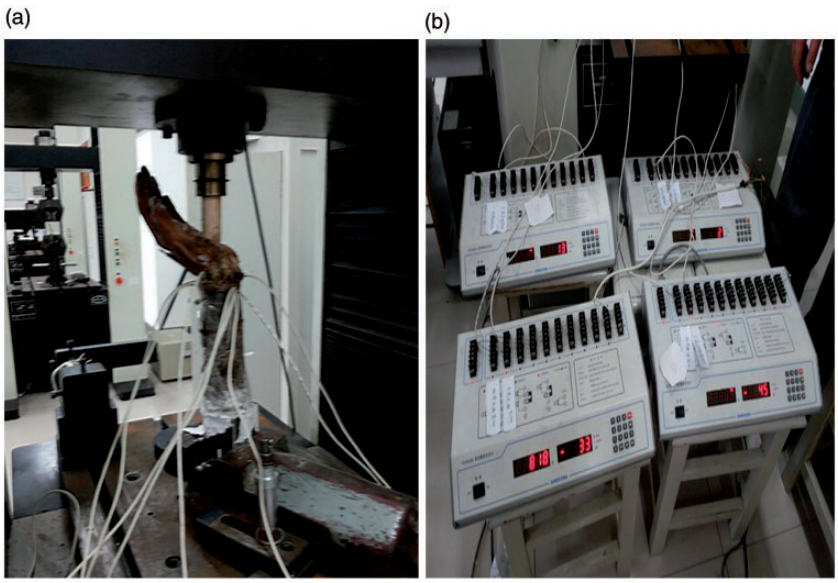

Figure 1. (a) The axial-loading experiment on cadaveric wrist specimens. (b) The establishment of four static strain test units.

Table 1. Comparison of the peak stress and declines between the experimental and control groups.

	Peak stress of the control group, MPa	Peak stress of the experimental group, MPa	Mean percentage decline in peak stress
Radial distal palmar unit	36.6	20.2	44.8%*
Ulnar distal palmar unit	37.9	24.3	35.9%*
Radial distal dorsal unit	9.4	5.7	39.4%*
Ulnar distal dorsal unit	13.4	4.8	64.2%*
Radial proximal palmar unit	58.5	30.1	48.5%*
Ulnar proximal palmar unit	37.4	24.9	33.4%*
Radial proximal dorsal unit	10.5	10.3	1.9%
Ulnar proximal dorsal unit	15.3	13.8	9.8%

Data presented as mean.
*Significant between-group difference ($P < 0.05$); paired Student's *t*-test.

forearm to the fingertip. During the process of scanning, the wrist was fixed with the direction of axial-loading and the posture maintained. It was determined that the established wrist model was set to 75° of dorsiflexion and 10° of pronation. The CT scan data were saved in Digital Imaging and Communications in Medicine format and input into Mimics 19.0 software (Materialise) to initially establish the three-dimensional (3D) geometric model of the wrist. The contours of the forearm cortex, loose tissue and surrounding soft tissue were extracted using thresholding and manual drawing tools. The stereolithography format data were obtained and input into the Geomagic Studio 12.0 software (Raindrop Geomagic). Deep level hole filling and smoothing for each part of the model was undertaken to prevent the occurrence of poor grids. Finally, the data that generated a solid 3D model were imported into Abaqus 6.51 software (Dassault Simulia) for statistical analysis.

Statistical analyses

All statistical analyses were performed using IBM SPSS Statistics for Windows, Version 22.0 (IBM Corp., Armonk, NY, USA). Between-group comparisons were undertaken using paired Student's *t*-test. A P-value < 0.05 was considered statistically significant.

Results

In the axial-loading simulated experiment for the control group, the stress magnitude and properties of the wrist model were different with the stress peaks of the palmar units being higher than those of the dorsal units (Table 1). The stresses of the palmar units were mainly manifested in the form of pressure. The initial stage of the dorsal units was manifested in the form of pressure, but the whole process was manifested in the form of tension. The equivalent stresses of the radial distal and proximal palmar units under 600 N load were 36.6 MPa and 58.5 MPa, respectively. Under the same loading conditions, the equivalent stresses of the ulnar distal and proximal palmar units were close to those on the radial distal and proximal palmar units, which were 37.9 MPa and 37.4 MPa, respectively. In all groups of units, the stresses of the dorsal units were all less than those of the palmar units. Moreover, the stresses of the ulnar distal and proximal dorsal units and the radioulnar proximal dorsal units were manifested

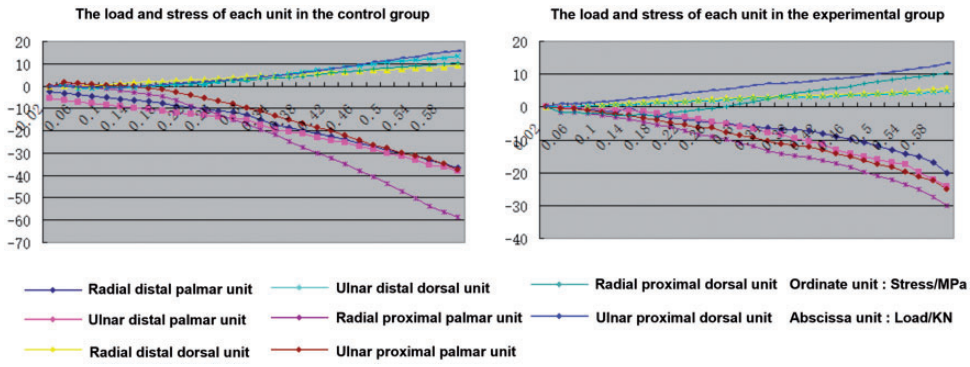

Figure 2. Comparison of the load and stress of each unit in the experimental and control groups. Data presented as mean. The colour version of this figure is available at: http://imr.sagepub.com.

in the form of pressure at the initial stage of the experiment, while manifested in the form of tension at the middle and late stages. The maximum stresses of the radioulnar distal dorsal units were 9.4 MPa and 13.4 MPa, while the maximum stresses of the radioulnar proximal dorsal units were 10.5 MPa and 15.3 MPa, respectively.

In the axial-loading simulated experiment for the experimental group, the stress magnitude and properties of the wrist model were different with the stress peaks of the palmar units being higher than those of the dorsal units (Table 1); and each unit was mainly manifested in the form of pressure. The initial stage of the radial proximal dorsal unit was manifested in the form of pressure, while manifested in the form of tension at the middle and late stages. In addition, tension was the main manifestation of the radioulnar distal, dorsal units and ulnar proximal dorsal unit. Under the same loading conditions of 600 N, the stresses of the radioulnar proximal palmar units were all higher than those of the radioulnar distal palmar units. The equivalent stresses of the radioulnar proximal palmar units under 600 N load were 30.1 MPa and 24.9 MPa, while the equivalent stresses of the radioulnar distal palmar units were 20.2 MPa and 24.3 MPa, respectively. In all groups of units, the stresses of the dorsal units were all less than those of the palmar units. The maximum stresses on the radioulnar distal dorsal units were 5.7 MPa and 4.8 MPa, while the maximum stresses on the radioulnar proximal dorsal units were 10.3 MPa and 13.8 MPa, respectively (Figure 2).

A comparison of the stress peaks and percentage declines between the two groups are presented in Table 1. In all eight units, except for the radioulnar proximal dorsal units, there were significant stress differences between the control and experimental groups at the late stage of the experiment ($P < 0.05$ for all comparisons). Overall, the stresses of the remaining six units in the experimental group were decreased by 44% compared with control group (Figure 3).

Based on the extension, flexion, retraction and rotation of a normal human wrist, the 3D finite element model (FEM) of the wrist was composed of 136 897 units of bone, 9166 units of cartilage and 228 893 units of soft tissue, totalling 374 956 units (Table 2).

The stress distribution in the models of the control and experimental groups at the late stage of the experiments are shown in Figure 4. The results of the 3D FEM analysis confirmed the conclusions of

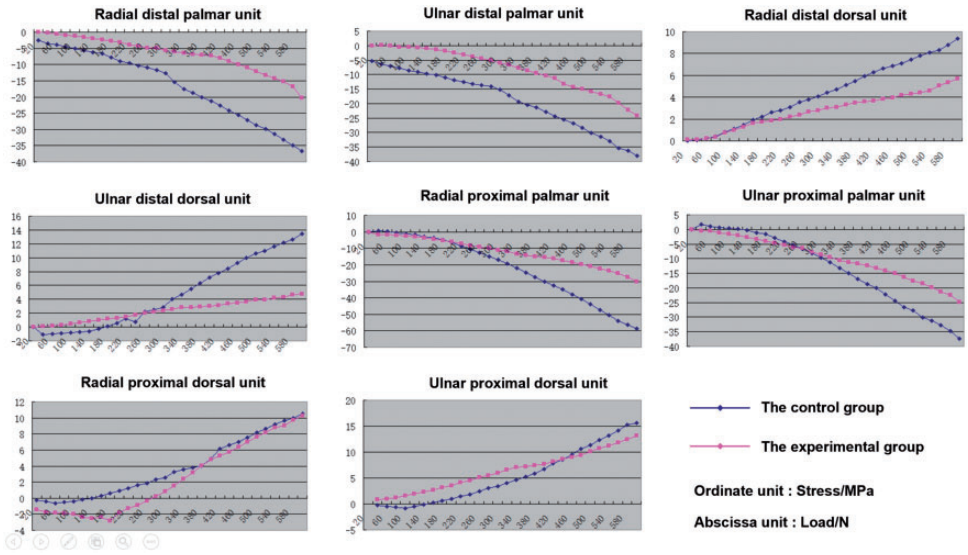

Figure 3. Comparison of the load and stress curves for each unit between the experimental and control groups. Data presented as mean. The colour version of this figure is available at: http://imr.sagepub.com.

Table 2. The number of nodes, unit types and unit numbers of the finite element model of a normal human wrist joint.

	Bone	Cancellous bone	Soft tissue	Rigid ground	Soft brace	Rigid brace
Unit number	136 897	9166	228 893	2500	12 048	3984
Nodes	228 808	20499	356 621	2603	4196	2090
Unit type	C3D10M	C3D10M	C3D10M	S4R	C3D10M	S3R

the biomechanical experiments described above. With the exception of the radioulnar proximal and dorsal units, there were no significant stress colour differences between the control and experimental groups at the end of the experiments. However, the stress colour of the remaining six units in the experimental group were lighter than those in the control group, indicating that the stresses of the experimental group were less than those of the control group.

Discussion

As the aging population continues to rise, there has been a concomitant increase in the number of elderly patients with wrist fractures.[14–16] This is particularly relevant to middle-aged and elderly women because of the negative impact that the menopause and oestrogen loss has on their bone health; and along with age-related declines in physical function and their ability to deal with emergencies, they are at a high risk of wrist fractures.[13,17–19] In addition, wrist fractures are also common in young and middle-aged people as a result of injuries caused by their daily exercise and work.[20,21] This study aimed to improve the prevention of wrist fractures in people of different ages by updating the poorly functioning wrist protectors that are currently available.

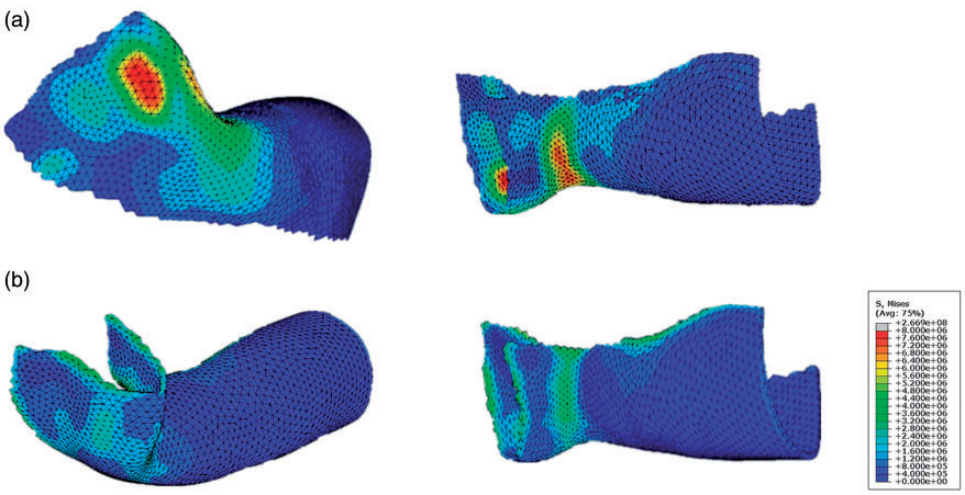

Figure 4. Stress distribution patterns in the 3-dimensional finite element models of the control and experimental groups at the late stage of the experiments: (a) the stress colour pattern of the control group that did not have the buffer of a wrist protector was deeper than the experimental group in the radioulnar distal palmar, radioulnar proximal palmar and radioulnar distal dorsal units; (b) the overall stress colour pattern of the experimental group that had a wrist protector was lighter than the control group. The colour version of this figure is available at: http://imr.sagepub.com.

This current study combined mechanical experiments using cadaveric wrists with FEA wrist simulation analysis to evaluate the ability of wrist protectors to protect against external forces from multiple angles.

During the current axial-loading experiments, it was found that despite the complex anatomical structure of the wrist joint, the external forces were mainly transmitted from the navicular and lunar bone down to the radioulnar joints; and then continued to the proximal end of the forearm. During this process, the radioulnar joint was considered to a composite joint and the compressive deformation occurred on the radioulnar palmar units, presenting as a compressive stress. The tensile deformation occurred on the radioulnar dorsal units, presenting as a tensile stress. In addition, under normal circumstances, during the deformation of the radioulnar joint under external forces, the palmar and dorsal units with the same axis distance had the same bending moments.[22] However, in this current experiment, the axial centre was biased to the dorsal units under the impact; and all units had larger palmar bending moments and smaller dorsal bending moments, which explains why the absolute stress peak values of the palmar units were greater than those of the dorsal units.

Based on the comparison of the two groups in the current study, it was found that wearing a wrist protector can effectively reduce the stress on the radioulnar distal palmar, radioulnar proximal palmar and radioulnar distal dorsal units, while having no obvious influence on the radioulnar proximal dorsal units. In the experimental group, the stresses of the radioulnar distal palmar and dorsal units were reduced by 44% compared with the control group, which was related to the absorption and shunting of the impact load on the wrist protector. Hence, when designing and improving wrist protectors, it would be reasonable to place the stress centre on the radioulnar distal palmar and dorsal units.

Similar to the findings of this current study, a previous study designed a hip protector and screened three volunteers that performed simulated human side fall tests.[23] The results indicated that mean peak impact force could reach 1738.88 ± 215.66 N in the group without a hip pad, while the mean peak impact force in the group with a hip pad increased to 1907.44 ± 441.42 N.[23] This result demonstrated that wearing a hip protector could increase the peak impact force on the hip, which might be able to prevent the occurrence of a hip fracture.

This current study had several limitations. First, the cadaveric specimens lacked the natural soft tissue tension and stress protective mechanisms of a living normal human body, so they were unable to accurately reflect the true stress and strain of the normal human wrist.[24–26] Secondly, the experimental sample size was only six, which was relatively small. Thirdly, the force mechanisms involved in causing a wrist fracture as a result of an external force impact are complex. However, this study was limited to vertical axial-loading of the wrist joint, which simplified the actual forces on the human body. Finally, the FEA method has certain limitations. The FEM simulation can only approximate to the real situation. The authenticity and validity of these preliminary results need to be verified with additional experiments.[27]

In conclusion, this current study demonstrated that the stresses on the radioulnar palmar units were high and manifested in the form of pressure; while the stresses on the radioulnar dorsal units were relatively lower and manifested in the form of tension. Under the physiological load, wearing a wrist protector reduced the stress on the radioulnar distal palmar, radioulnar proximal palmar and radioulnar distal dorsal units, while it had no obvious influence on the radioulnar proximal dorsal units. When designing and improving wrist protectors, it would be reasonable to place the stress centre on the radioulnar distal palmar and dorsal units.

Declaration of conflicting interest

The authors declare that there are no conflicts of interest.

Funding

This research received funding from the Major Project of Changzhou Health Committee (no: ZD201715).

ORCID iD

Yan-Hui Pei https://orcid.org/0000-0001-5161-2427

References

1. de Putter CE, Selles RW, Polinder S, et al. Epidemiology and health-care utilisation of wrist fractures in older adults in The Netherlands, 1997-2009. *Injury* 2013; 44: 421–426.
2. Gregson CL, Carson C, Amuzu A, et al. The association between graded physical activity in postmenopausal British women, and the prevalence and incidence of hip and wrist fractures. *Age Ageing* 2010; 39: 565–574.
3. Jung HY, Chang M, Kim KM, et al. Effect of Wrist Joint Restriction on Forearm and Shoulder Movement during Upper Extremity Functional Activities. *J Phys Ther Sci* 2013; 25: 1411–1414.
4. Park K, Chang PH and Kang SH. In Vivo Estimation of Human Forearm and Wrist Dynamic Properties. *IEEE Trans Neural Syst Rehabil Eng* 2017; 25: 436–446.
5. Erhart S, Lutz M, Arora R, et al. Measurement of intraarticular wrist joint biomechanics with a force controlled system. *Med Eng Phys* 2012; 34: 900–905.
6. Schreck MJ, Kelly M, Canham CD, et al. Techniques of Force and Pressure Measurement in the Small Joints of the Wrist. *Hand (N Y)* 2018; 13: 23–32.
7. Kramer A, Allon R, Wolf A, et al. Anatomical Wrist Patterns on Plain

Radiographs. *Curr Rheumatol Rev* 2019; 15: 168–171.
8. Crandall CJ, Hovey KM, Cauley JA, et al. Wrist Fracture and Risk of Subsequent Fracture: Findings from the Women's Health Initiative Study. *J Bone Miner Res* 2015; 30: 2086–2095.
9. Gallagher JC. Advances in osteoporosis from 1970 to 2018. *Menopause* 2018; 25: 1403–1417.
10. Gong H, Zhang M, Fan Y, et al. Relationships between femoral strength evaluated by nonlinear finite element analysis and BMD, material distribution and geometric morphology. *Ann Biomed Eng* 2012; 40: 1575–1585.
11. Palacios S, de Villiers TJ, Nardone FDC, et al. Assessment of the safety of long-term bazedoxifene treatment on the reproductive tract in postmenopausal women with osteoporosis: results of a 7-year, randomized, placebo-controlled, phase 3 study. *Maturitas* 2013; 76: 81–87.
12. Palacios S, Silverman SL, De Villiers TJ, et al. A 7-year randomized, placebo-controlled trial assessing the long-term efficacy and safety of bazedoxifene in postmenopausal women with osteoporosis: effects on bone density and fracture. *Menopause* 2015; 22: 806–813.
13. Belaid D, Vendeuvre T, Bouchoucha A, et al. Utility of cement injection to stabilize split-depression tibial plateau fracture by minimally invasive methods: A finite element analysis. *Clin Biomech (Bristol, Avon)* 2018; 56: 27–35.
14. Antoniadou E, Kouzelis A, Diamantakis G, et al. Characteristics and diagnostic workup of the patient at risk to sustain fragility fracture. *Injury* 2017; 48: S17–S23.
15. Frontera WR. Physiologic Changes of the Musculoskeletal System with Aging: A Brief Review. *Phys Med Rehabil Clin N Am* 2017; 28: 705–711.
16. Walters S, Khan T, Ong T, et al. Fracture liaison services: improving outcomes for patients with osteoporosis. *Clin Interv Aging* 2017; 12: 117–127.
17. Gallagher JC, Palacios S, Ryan KA, et al. Effect of conjugated estrogens/bazedoxifene on postmenopausal bone loss: pooled analysis of two randomized trials. *Menopause* 2016; 23: 1083–1091.
18. Khan A and Fortier M. Osteoporosis in menopause. *J Obstet Gynaecol Can* 2014; 36: 839–840.
19. Stagraczynski M, Kulczyk T, Leszczynski P, et al. Number of teeth and hormonal profile of postmenopausal women with osteoporosis, osteopenia and normal bone mineral density–a preliminary study. *Pol Merkur Lekarski* 2015; 39: 214–218 [Article in Polish, English abstract].
20. Beerekamp MSH, de Muinck Keizer RJO, Schep NWL, et al. Epidemiology of extremity fractures in the Netherlands. *Injury* 2017; 48: 1355–1362.
21. Clement ND, Duckworth AD, Wickramasinghe NR, et al. Does socioeconomic status influence the epidemiology and outcome of distal radial fractures in adults? *Eur J Orthop Surg Traumatol* 2017; 27: 1075–1082.
22. Sherman KM, Miller GJ, Wronski TJ, et al. The effect of training on equine metacarpal bone breaking strength. *Equine Vet J* 1995; 27: 135–139.
23. Sun P, Ouyang J. Prospect and current research on hip protector. *Zhongguo Xiu Fu Chong Jian Wai Ke Za Zhi* 2012; 26: 41–45 [Article in Chinese, English abstract].
24. Hogel F, Mair S, Eberle S, et al. Distal radius fracture fixation with volar locking plates and additional bone augmentation in osteoporotic bone: a biomechanical study in a cadaveric model. *Arch Orthop Trauma Surg* 2013; 133: 51–57.
25. Kang L, Dy CJ, Wei MT, et al. Cadaveric Testing of a Novel Scapholunate Ligament Reconstruction. *J Wrist Surg* 2018; 7: 141–147.
26. Mirarchi AJ, Hoyen HA, Knutson J, et al. Cadaveric biomechanical analysis of the distal radioulnar joint: influence of wrist isolation on accurate measurement and the effect of ulnar styloid fracture on stability. *J Hand Surg Am* 2008; 33: 683–690.
27. Sannino G and Barlattani A. Mechanical evaluation of an implant-abutment self-locking taper connection: finite element analysis and experimental tests. *Int J Oral Maxillofac Implants* 2013; 28: e17–e26.